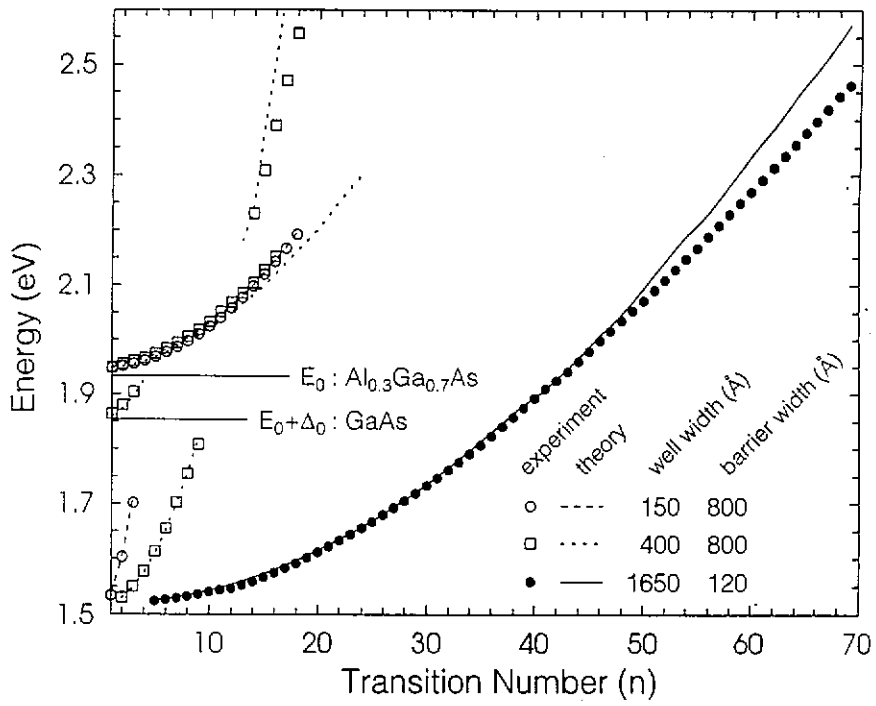

Fig. 11. Transitions energies vs. transition number for three surface QWs. The index n corresponds to a transition between the nth heavy hole level and the nth conduction band level. All three samples have a GaAs cap layer grown on top of a $Al_{0.3}Ga_{0.7}As$ SQB (From Ref. 178).

As we might by now expect, superlattice structures also display above-barrier localized states.[119,186–188] In other words, wavefunction localization in the barrier layers above the barrier energy is a fairly universal property. Finite element calculations were performed for the superlattice energy bands and for the wavefunctions for a 50 Å/50 Å GaAs/AlGaAs superlattice. The third mini-subband in the superlattice is the first band above the barrier in this case. Figure 12 shows quite clearly the localization of this wavefunction in the barrier layers of the superlattice. The probability density for states with the superlattice wavevector $q_z = (0, 0.5, 1)$ are given, illustrating that the localization is active throughout the superlattice Brillouin zone. States belonging to the next higher miniband are found to have two peaks in the probability density in the barrier layer, corresponding to the second excited state above the barrier band edge, and so on.

Effects of external perturbations on the surface QW states, SQB states, and above-barrier states are clearly of interest with regard to novel physical issues as well as for their promise in optoelectronics. In conclusion, the theoretical analysis using FEM has provided a clear and unambiguous interpretation of the transitions observed in modulated reflectivity spectra for SQW structures; in fact, feasibility studies using the FEM were performed before the structures were grown.

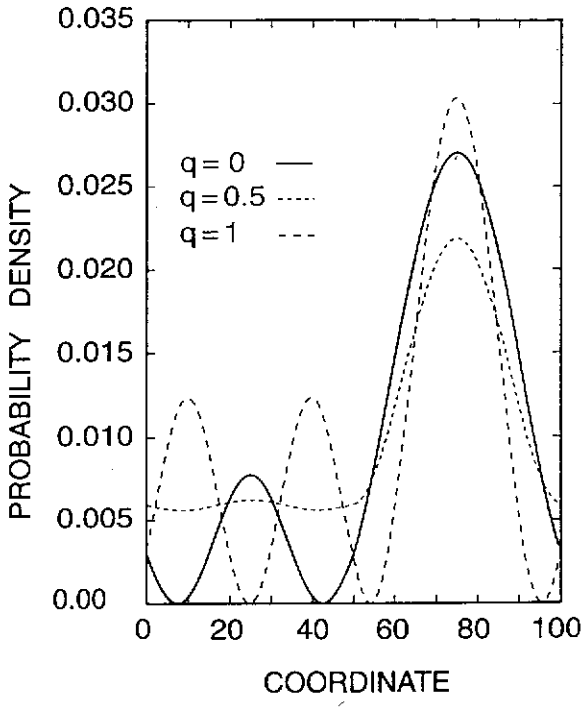

Fig. 12. Probability density for conduction electrons in the third mini-subband of a 50 Å/50 Å GaAs/$Al_{0.33}Ga_{0.67}As$ superlattice, displaying the localization in the barrier region.

5. Applications of Wavefunction Engineering – Quantum Wires and Quantum Wire Superlattices

5.1. *Bound States in a Rectangular Quantum Wire*

In 1980, Sakaki[192] considered theoretically the consequences of growing heterostructures which would confine electrons in two dimensions, the so-called quantum wire (which we will denote by 'quantum well wire' or QWW) or the two-dimensional quantum well. Since then, control over growth at an atomic level has allowed the fabrication of such heterostructures.[193,194] As in one dimensional confinement, the principal effect is to profoundly change the energy spectra of electrons which in turn influence the optical and transport properties of the composite material.[195–200]

We consider the calculation of electron and hole energy levels in a GaAs quantum wire with a finite confining potential arising from the band offset of the surrounding AlGaAs medium. Earlier theoretical considerations have either assumed that the confining potential is infinite,[197–200] or have used a periodic arrangement of QWWs which converts the problem to the determination of narrow energy bands in a periodic structure using tight-binding models.[201,202] Our results show that the energy levels for the finite potential are significantly lower than those obtained with

the infinite barrier, which suggests that the infinite barrier approximation is not valid for quantum wires. More striking, however, is that when a finite barrier potential is used in calculating the energy spectrum for a quantum wire with square cross-section, there is a lifting of the degeneracies of certain levels.

The FEM has been used to solve the Schrödinger equation in the effective mass approximation for $GaAs/Ga_{0.63}Al_{0.37}As$ QWWs of typical dimensions. Group theoretical arguments are used to explain which of the degeneracies present in the infinite square well should be lifted when a finite barrier is used. We will also discuss the dependence of the heavy-hole doublet splitting on the barrier height for a range of concentrations x in the $Al_xGa_{1-x}As$ barriers.

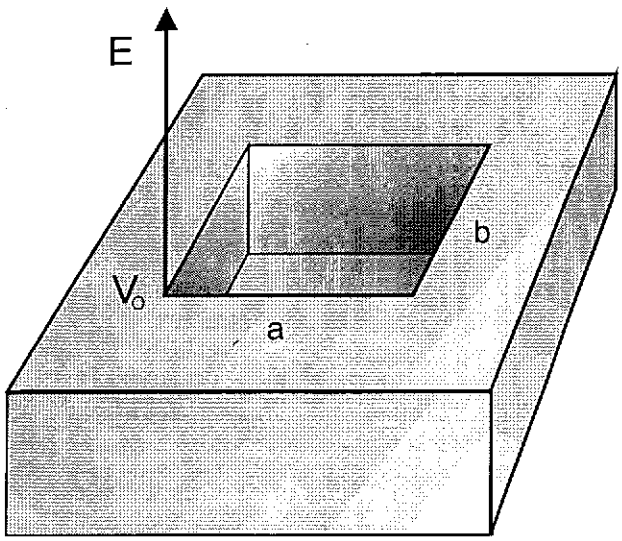

Fig. 13. The finite-barrier potential energy function giving rise to two-dimensional confinement in a quantum wire.

5.1.1. *Finite Element Analysis of the Quantum Wire*

In the envelope function approximation,[16,17] the most general form of the differential equation for the electron's QWW envelope function $f(x, y)$ contains a nonseparable potential $V(x, y)$ corresponding to a finite barrier height (see Fig. 13):

$$-(\hbar^2/2m^*)(\partial^2/\partial x^2 + \partial^2/\partial y^2)f(x, y) + V(x, y)f(x, y) = Ef(x, y), \qquad (6)$$

where the carrier effective mass m^* is m_w^* or m_b^* in the well or barrier, respectively. Assuming a rectangular-well wire of dimension $a \times b$ centered at the origin, the 'kitchen-sink' potential is $V(x, y) = 0$ for $|x| \leq a/2$ and $|y| \leq b/2$, and $V = V_0$ outside the well. The input parameters for the band offsets and conduction electron, light hole, and heavy hole effective masses in GaAs and in AlGaAs are obtained in the same way as in earlier investigations using the Bastard model.[32]

The FEM procedure employed to solve Eq. (6) for the energy levels as well as the eigenfunctions $f(x, y)$ is an extension of the approach discussed in Sec. 2 for the case of confinement along only one axis. The region of interest is partitioned into small elements, and the as-yet-unknown function $f(x, y)$ in each element is approximated by local Hermite interpolation functions. The global function $f(x, y)$ is constructed by joining the locally defined interpolation functions and requiring that $f(x, y)$ and its derivatives be continuous across the element boundaries. As mentioned earlier, in the FEM it is quite easy to implement the boundary condition at the well-barrier interface, which requires the continuity of both $f(x, y)$ and the effective mass derivative. The resultant eigenvalue problem is solved for the energy spectra and the values of f, $\partial f/\partial x$, $\partial f/\partial y$, and $\partial^2 f/\partial x \partial y$ at the nodes. Details of the two-dimensional FEM are given in Ref. 24.

Table 1. Conduction electron energy levels in $GaAs/Al_{0.37}Ga_{0.63}As$ QWs, with $m_w^* = 0.0665\ m_0$ and $m_b^* = 0.0858\ m_0$, for states with quantum numbers (n_x, n_y), (After Ref. 26).

Cross-sectional area $a \times b$ (Å^2)	Energy (meV) $V_0 = 276$ meV	(n_x, n_y)	Energy (meV) $V_0 = \infty$	(n_x, n_y)
50 × 50	155.3	(1,1)	452.4	(1,1)
100 × 50	111.1	(1,1)	282.7	(1,1)
	197.6	(2,1)	452.4	(2,1)
100 × 100	63.5	(1,1)	113.1	(1,1)
	155.2	(1,2)	282.7	(1,2)
	155.2	(2,1)	282.7	(2,1)
	239.6	(2,2)	452.4	(2,2)
	274.2	(1,3) + (3,1)	565.5	(1,3)

Table 2. Light hole energy levels in $GaAs/Al_{0.37}Ga_{0.63}As$ QWs, with $m_w^* = 0.0905\ m_0$ and $m_b^* = 0.1107\ m_0$, (After Ref. 26).

Cross-sectional area $a \times b$ (Å^2)	Energy (meV) $V_0 = 184$ meV	(n_x, n_y)	Energy (meV) $V_0 = \infty$	(n_x, n_y)
50 × 50	110.7	(1,1)	332.4	(1,1)
100 × 50	79.8	(1,1)	207.8	(1,1)
	141.3	(2,1)	332.4	(2,1)
100 × 100	46.0	(1,1)	83.1	(1,1)
	111.7	(1,2)	207.8	(1,2)
	111.7	(2,1)	207.8	(2,1)
	171.0	(2,2)	332.4	(2,2)

Table 3. Heavy hole energy levels in $GaAs/Al_{0.37}Ga_{0.63}As$ QWs, with $m_w^* = 0.3774\ m_0$ and $m_b^* = 0.3865\ m_0$, (After Ref. 26).

Cross-sectional area $a \times b$ (Å^2)	Energy (meV) $V_0 = 184$ meV	(n_x, n_y)	Energy (meV) $V_0 = \infty$	(n_x, n_y)
50 × 50	46.5	(1,1)	79.7	(1,1)
	112.2	(1,2)	199.3	(1,2)
	112.2	(2,1)	199.3	(2,1)
	172.7	(2,2)	318.8	(2,2)
100 × 50	30.9	(1,1)	49.8	(1,1)
	53.1	(2,1)	79.7	(2,1)
	89.5	(3,1)	129.5	(3,1)
	97.4	(1,2)	169.4	(1,2)
	119.0	(2,2)	199.3	(2,2)
	138.2	(4,1)	199.3	(4,1)
	154.0	(3,2)	249.1	(3,2)
	182.8	(1,3) + (5,1)	288.9	(5,1)
100 × 100	15.1	(1,1)	19.9	(1,1)
	37.4	(1,2)	49.8	(1,2)
	37.4	(2,1)	49.8	(2,1)
	59.7	(2,2)	79.7	(2,2)
	74.0	(1,3) + (3,1)	99.6	(1,3)
	74.2	(1,3) − (3,1)	99.6	(3,1)
	96.2	(2,3)	129.5	(2,3)
	96.2	(3,2)	129.5	(3,2)
	123.4	(1,4)	169.4	(1,4)
	123.4	(4,1)	169.4	(4,1)
	132.2	(3,3)	179.4	(3,3)
	144.2	(2,4) + (4,2)	199.3	(2,4)
	145.9	(2,4) − (4,2)	199.3	(4,2)
	179.4	(3,4)	249.1	(3,4)
	179.4	(4,3)	249.1	(4,3)
	178.32	(1,5) + (5,1)	259.1	(1,5)
	179.70	(1,5) − (5,1)	259.1	(5,1)

In Tables 1–3, we give the FEM values[26] for the energy levels (accurate to within 0.1 meV) of conduction electrons, light holes, and heavy holes in GaAs/$Ga_{0.63}Al_{0.37}As$ rectangular wires of dimension 50 Å × 50 Å, 100 Å × 50 Å, and 100 Å × 100 Å. A conduction band offset of 0.6 ΔE_g at the hetero-interface was used in the calculations. As in the case of one-dimensional quantum well confinement, it is convenient to label the energy levels using the quantum numbers (n_x, n_y) associated with the infinite well, where n_x and n_y are the quantum numbers for the one-dimensional infinite square well in the x and y direction. The energy levels obtained using the infinite-barrier approximation are also included in Tables 1–3 for

comparison. Note that all of the energy levels are lowered from the values obtained with an infinite barrier. The effect of the finite potential is greater for small a and b, and for energy levels approaching V_0. For the 50 Å × 50 Å QWW, the single bound state of the conduction electron and of the light hole are reduced in energy by a factor of three from the infinite barrier result. Clearly, the infinite barrier approximation is invalid in this case.

Wavefunctions for three low-lying heavy hole states in a 100 Å × 100 Å QWW are shown in Fig. 14. As expected, the FEM wavefunctions are similar to their infinite well analogs except that they leak out into the classically forbidden barrier region. The amount of barrier penetration increases as the energy level approaches the barrier height.

Note that the degeneracy for the (2,2) and (4,1) states of the infinite rectangular well (100 Å × 50 Å) is removed. This degeneracy is present only in the infinite well because the energy is simply related to the dimension of the well and the quantum number, and the rectangular well was chosen to have commensurate sides. It is also interesting to note that there is a mixing of the states (5,1) and (1,3) for the finite rectangular well. The state lower in energy is predominantly (1,3), and the state which is slightly higher in energy is predominantly (5,1). For an Al composition of $x = 0.37$ in the barriers, only the lower state is bound, and its energy is reported in Table 6. However, for a composition $x = 0.4$, both states are bound and the FEM wavefunctions exhibit this mixing of states. Such mixing can be expected only if two states that are close in energy have the same symmetry in x and y. Of course, this mixing will depend on the dimensions of the rectangular well.

We note that currently available quantum wires have typical dimensions on the order of 1000 Å, for which we would expect finite-barrier effects to be less pronounced than in the examples shown in Table 1–3. We have calculated the energy levels of conduction electrons in a square quantum wire of dimension 1000 Å, using a finite barrier of 276 meV. The first few levels are lowered by about 5 % from the value obtained in the infinite barrier approximation. The effect is naturally accentuated for higher levels as they approach the barrier height V_0.

5.1.2. *Symmetry Properties of the Square Quantum Wire*

The symmetry properties of the envelope functions for the squared quantum wire are governed by the symmetry of the potential, C_{4v}. The character table for C_{4v} is given in Ref. 203. For this group, the effects of the operators $\{E, C_2, 2C_4, 2\sigma_v, 2\sigma_d\}$ on the function $f(x, y)$ are:

$$
\begin{aligned}
Ef(x, y) &= f(x, y) \quad , \quad C_2 f(x, y) = f(-x, -y)\,, \\
C_4 f(x, y) &= f(y, -x) \quad , \quad C_4^{-1} f(x, y) = f(-y, x)\,, \\
\sigma_v f(x, y) &= f(-x, y) \quad , \quad \sigma_v^{-1} f(x, y) = f(x, -y)\,, \\
\sigma_d f(x, y) &= f(y, x) \quad , \quad \sigma_d^{-1} f(x, y) = f(-y, -x)\,.
\end{aligned}
$$

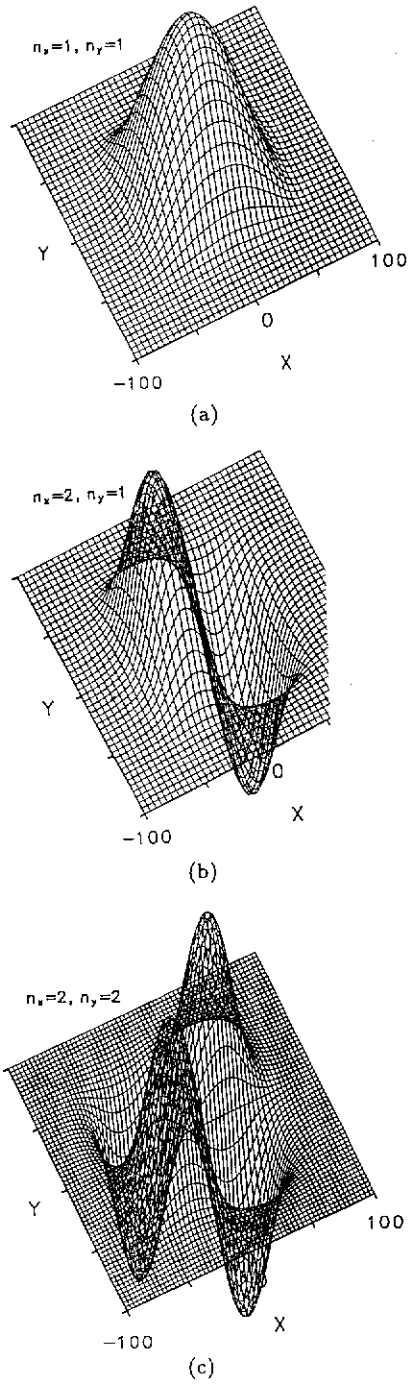

Fig. 14. Heavy hole wavefunctions in a 100 Å × 100 Å QW for (a) the ground state (1,1); (b) the first excited state (2,1); and (c) the excited state (2,2), (From Ref. 26).

It is straightforward to determine the representation corresponding to the infinite well eigenfunctions (n_x, n_y). The (odd, odd) singlet states with $n_x = n_y$ belong to the A_1 representation and the (even, even) singlet states belong to B_2. The degenerate states with $n_x \neq n_y$ can be classified as follows:

$$\begin{array}{rr} (\text{even, odd}) \text{ and } (\text{odd, even}) & E \\ (\text{even, even}) & A_2 + B_2 \\ (\text{odd, odd}) & A_1 + B_1 \end{array}$$

Since the (even, even) and (odd, odd) degenerate states are combinations of two distinct irreducible representations, the degeneracy of these levels is not a consequence of the symmetry group of the square, but rather is due to the separability of the infinite square well potential. Using linear combinations of the standard (n_x, n_y) eigenfunctions it is possible to construct eigenfunctions which correspond to one of the one-dimensional irreducible representations A_1, A_2, B_1, or B_2. For example, (1,3) + (3,1) transforms as A_1 and (1,3) − (3,1) transforms as B_1. As we shall see, these are a more natural choice for the basis functions of this 2-dimensional subspace in that they are the $V_0 \to \infty$ limit of the finite barrier eigenfunctions.

For finite barriers, the potential is nonseparable and the accidental degeneracy which was present in the infinite barrier case for the (even, even) and (odd, odd) levels is lifted (see Table 6).

The state that is antisymmetric about the diagonal of the square (B_1, A_2) is less bound than its symmetric counterpart (A_1, B_2). As expected, the splitting of these particular energy levels decreases as the barrier height increases, and in the limit $V_0 \to \infty$ the states are truly degenerate. In Fig. 15, we show this dependence of level splitting on barrier height for heavy holes in a 100 Å × 100 Å GaAs/AlGaAs wire for the compositional range $0.1 > x > 0.4$. In some cases, the splitting of the doublet results in one state being bound, and the other free; for example, at $x = 0.1$, the state (1,3) + (3,1) is bound, but (1,3) − (3,1) is unbound. Also note that the energy levels for the (1,5) ± (5,1) actually cross over the (3,4) level; hence, even the ordering of the energy levels is a function of V_0.

The FEM wavefunctions for the square well with finite barrier are similar to their infinite barrier analogs except that there is penetration of $f(x, y)$ into the barrier region. For the degenerate states of the E representation, any two orthogonal states which span the subspace are acceptable eigenstates. In cases where the degeneracy is removed, the wavefunctions for the finite barrier must correspond to a single representation as required by the group properties; the wavefunctions are either even or odd with respect to reflection through the diagonals. The FEM wavefunctions for the states (1,3) + (3,1) and (1,3) − (3,1) are shown in Fig. 16 over a single quadrant $(x, y \geq 0)$ for clarity of presentation; the antisymmetric state vanishes at all $x = y$ as expected.

By studying the symmetry properties of the confining potential, it is straightforward to predict which of the degeneracies present in the infinite barrier approximation are due to the separability of the potential, and hence are accidental and will be

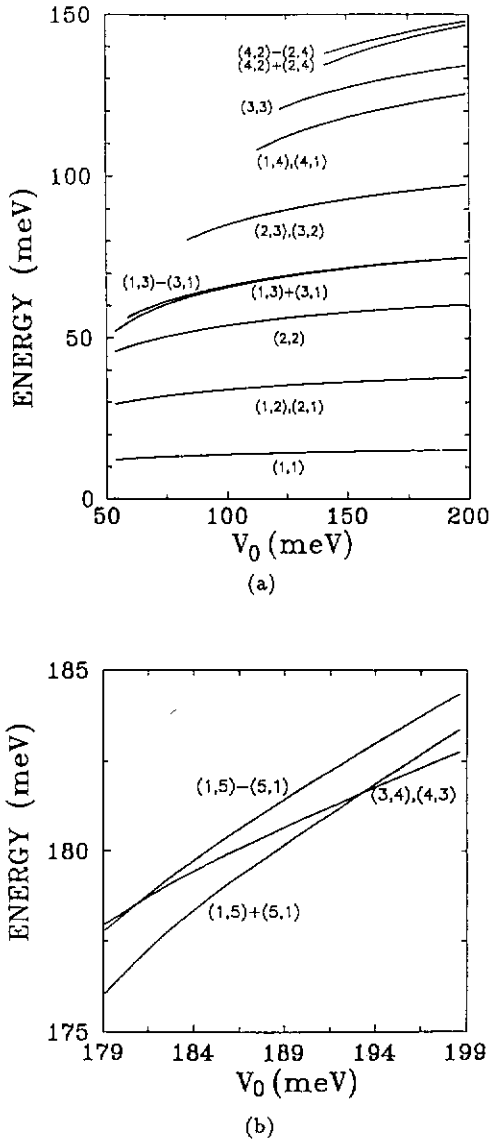

Fig. 15. The dependence of heavy hole energy levels on the barrier height in a 100 Å × 100 Å QW for (a) the first 10 energy levels and (b) for levels 11–13 (From Ref. 26).

removed in the presence of a finite barrier. One can also apply this analysis to the more interesting case of the three dimensional quantum cubic dot, where the lowest 40 levels of the infinite-barrier spectrum contain at most three-, six-, nine- and twelve-fold degeneracies. Degeneracies that arise from non-identical quantum numbers [for example, (2,2,5) and (4,4,1)] are automatically broken for a finite barrier since the energy is no longer simply related to the quantum numbers. The other degenerate states for the infinite-barrier quantum cubic dot can be analyzed by

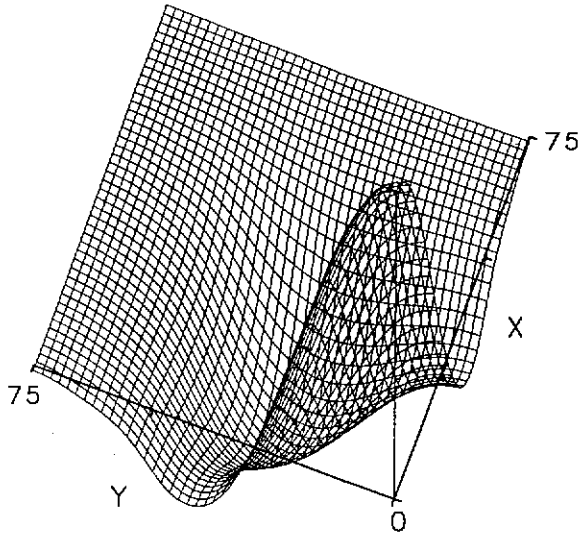

$(n_x, n_y) = (3, 1) + (1, 3)$

(a)

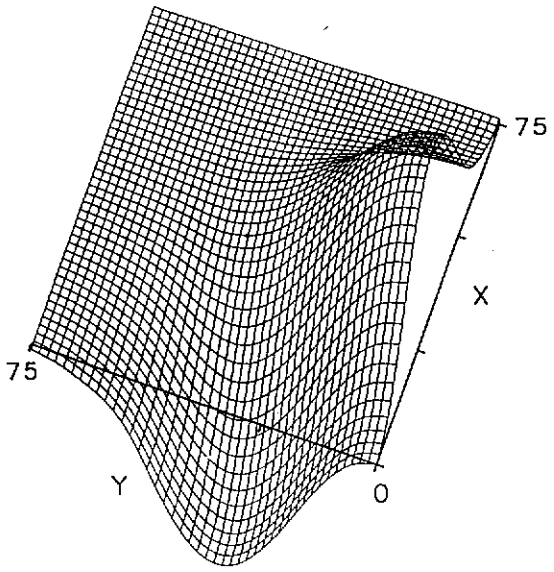

$(n_x, n_y) = (3, 1) - (1, 3)$

(b)

Fig. 16. Heavy hole wavefunctions in a 100 Å × 100 Å QW for (a) the excited state (1,3) + (3,1), and (b) the excited state (1,3) − (3,1), in the first quadrant (From Ref. 26).

looking at the behavior of the analytic solutions under the operations for the cubic group O_h. Since all of the representations O_h are one-, two- or three-dimensional,[203] the energy spectra for the finite-barrier quantum dot can have at most three-fold degeneracies. Consequently, the spectrum for the finite-barrier will contain many doublets and triplets whose splitting depends on the barrier heights.

The FEM provides realistic numbers for the energy spectra in rectangular quantum wires. Such accuracy is crucial in the study of linear and nonlinear optical properties of semiconductor heterostructures. In particular, the infinite-barrier approximation is invalid and leads to serious errors in both the qualitative and quantitative aspects of the energy spectra. The FEM can readily be applied to two-dimensional confinement problems where the effective mass and the potential are more complicated functions of the coordinates; it is also possible to accommodate any cross-sectional configuration, including QWWs grown on grooves. It is obvious that wavefunction engineering has tremendous potential in device applications based on two-dimensional carrier confinement.

5.2. *Two-Dimensional Stacking of Quantum Wires—The Checkerboard Superlattice*

Recent progress in the fabrication of QWWs with electronic confinement in two dimensions suggests that the growth of periodic structures of quantum wires will eventually become feasible. The micro-fabrication advances already achieved and the novel optoelectronic properties expected from such structures have motivated us to study a quantum structure consisting of rectangular semiconductor wires (of GaAs and AlGaAs, for example), stacked alternately and having the two-dimensional periodicity shown in Fig. 17. In the following we refer to this as a checkerboard superlattice (CBSL).[27] Here we will consider the effects of carrier wavefunction overlap across the barriers in the directions parallel to the CBSL axes, and the free-carrier induced nonlinear optical properties of such a structure with carriers in the lowest conduction miniband.

We first obtain the energy minibands for conduction electrons moving in the periodic CBSL confining potential, shown in Fig. 18, arising from the (finite) conduction band offset of AlGaAs with respect to GaAs. These results are then used to obtain the optical nonlinearity for radiation propagating along the longitudinal (z) axis of the wires, with electric fields being either along the x or the y directions. It has been demonstrated that band nonparabolicity induces a nonvanishing third order nonlinear optical susceptibility, $\chi^{(3)}$, in bulk semiconductors[204,205] and in superlattices.[206–210] We evaluate the free-carrier induced optical nonlinearity due to the band nonparabolicity generated by the Brillouin zone folding of the CBSL conduction band in *two directions*. The recent analysis[209] of the optical nonlinearity in planar superlattices has revealed, contrary to expectations, that superlattices with wider wells and/or barriers have larger values of $\chi^{(3)}$. This is reconfirmed here for the particular case investigated.

,3) + (3,1),

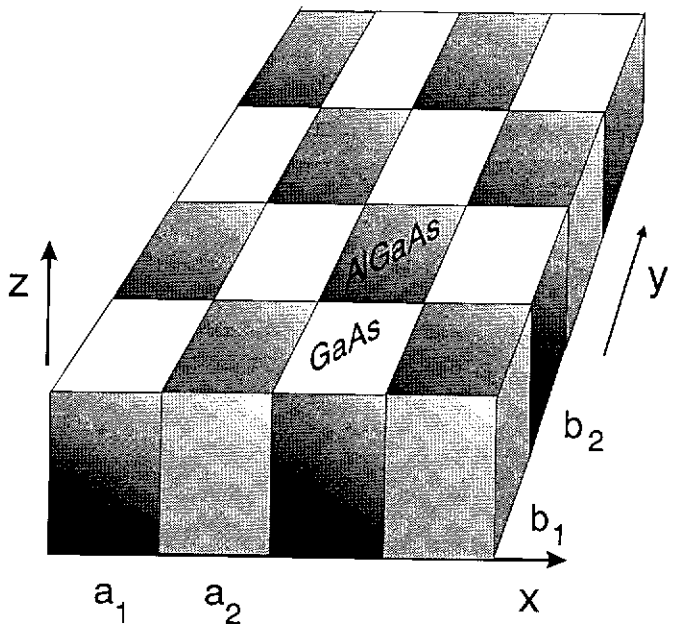

Fig. 17. The checkerboard superlattice: a stacking of quantum wires of GaAs and AlGaAs with periodicity along the x and y directions.

In the envelope function approximation, we again solve Schrödinger's equation given by Eq. (6) for the energy E, using $m_w^* = 0.0665\ m_0$ in the GaAs wells and or $m_b^* = 0.0858\ m_0$ in the $Ga_{0.7}Al_{0.3}As$ barriers. The non-separable potential $V(x, y)$ corresponds to a finite barrier height ($V_0 = 0.274$ eV) in the AlGaAs region.

The well and barrier thicknesses along the x and y directions are taken to be (a_1/a_2) and (b_1/b_2) respectively, with periodicities of lengths $a = a_1 + a_2$ and $b = b_1 + b_2$ expressed in units of $d = 5.642$ Å (the lattice parameter of GaAs).

Again, the boundary conditions imposed on the solutions are the continuity of the envelope functions $f(x, y)$ and the continuity of $(1/m^*)f'(x, y)$ across all interfaces. In addition, Bloch's conditions

$$f(a, y) = e^{ik_x a} f(0, y)\,;\ f(x, b) = e^{ik_y b} f(x, 0)\,, \tag{7}$$

are imposed to account for the super-translational symmetry of the CBSL.

Equation (6) has been solved subject to these two-dimensional boundary conditions using the FEM as discussed above. Here the basic 'unit cell' of the CBSL of dimensions $a \times b$ is split up into a number of elements, where the *hetero-interface* boundary conditions and Bloch's periodicity conditions mentioned above are easily incorporated into the FEM. The resultant global eigenvalue problem is solved for the eigenenergies for each value of $(k_x, k_y) \equiv [(\pi/a)q_x,\ (\pi/b)q_y]$ to obtain the energy bands. Figure 19 shows results for a CBSL of dimensions (6/4) along x and

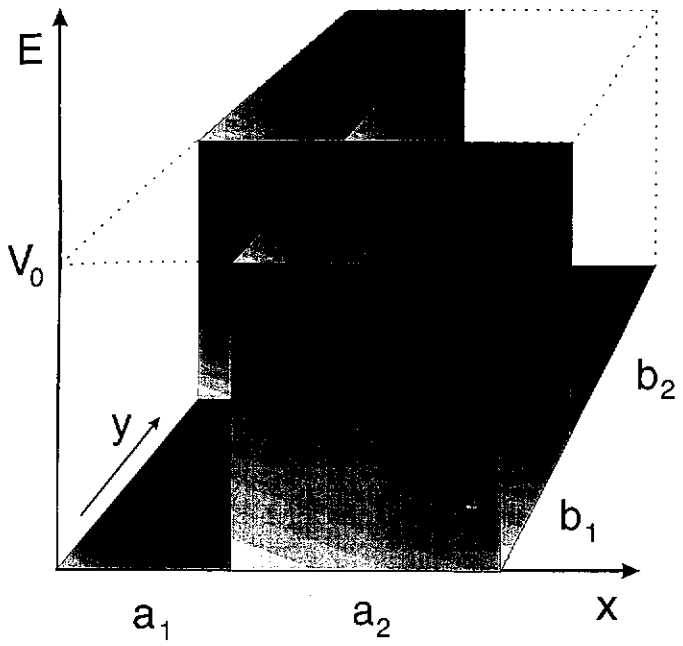

Fig. 18. The conduction band edge profile for the checkerboard superlattice shown over one period along the x and y directions.

(8/5) along y. For comparison, we have displayed the lowest energy mini-bands for planar superlattices of GaAs/AlGaAs. The band edges at $q = 0$ are lower in the planar structures because there the carriers are confined only in one direction. Note that the bands in the CBSL do not arise from a simple additive effect from the planar superlattice bands. Conduction electron wavefunctions for the first and the second minibands at the superlattice zone center and for the second miniband at the point $(q_x, q_y) = (1, 1)$ are shown in Fig. 20.

We now evaluate[27] the optical nonlinearity $\chi^{(3)}$ due to the carrier band non-parabolicity.[204,205] The nonlinear susceptibility $\chi_i^{(3)}$, $(i = x, y)$ is given by

$$\chi_i^{(3)} = -\frac{e^4 n\langle \partial^4 E/\partial k_i^4 \rangle}{24\hbar^4 \omega_1 \omega_2 \omega_3 (\omega_1 + \omega_2 - \omega_3)}, \tag{8}$$

where ω_1 and ω_2 correspond to incoming CO_2 laser beams in a 4-wave mixing experiment with photon wavelengths of $\lambda = 10.6$ μm, ω_3 corresponds to photons with $\lambda = 9.2$ μm, and the outgoing photon has energy $\hbar(\omega_1 + \omega_2 - \omega_3)$. The index i refers to the electric field polarizations in the x or the y directions.

The nonlinearity $\chi_i^{(3)}$ is proportional to the fourth derivative $\partial^4 E/\partial k^4$ averaged over the Fermi distribution of the carriers:

$$n\langle \partial^4 E/\partial k_i^4 \rangle = [2/(2\pi)^3] \int d^3k \partial^4 E/\partial k_i^4 f(E_F, E, T). \tag{9}$$

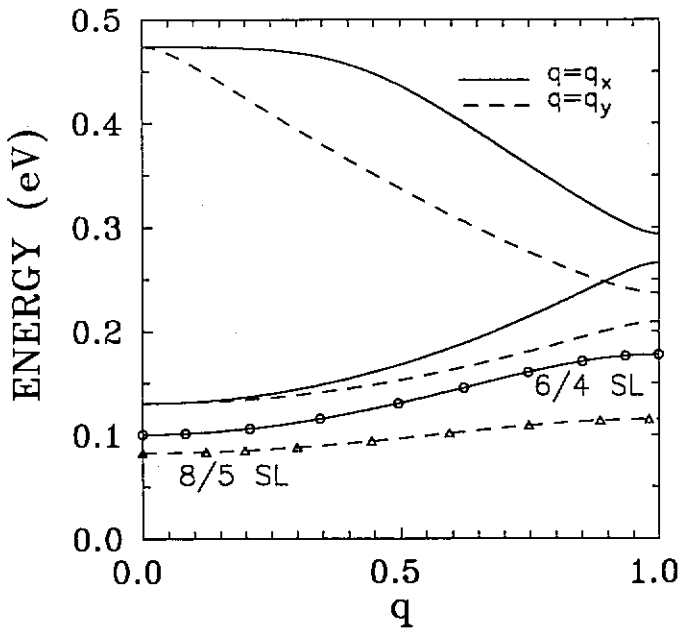

Fig. 19. The lowest two conduction minibands for a CBSL with well and barrier thicknesses of (6/4) and (8/5) (in units of $d = 5.642$ Å) along x (full curves) and along y (dashed curves), respectively. For comparison, the lowest minibands for 6/4 (full curve with open circles) and 8/5 (dashed curve with open triangles) planar superlattices are also shown (From Ref. 27).

At $T = 0$ K, the Fermi function $f(E_F, E, T)$ reduces to a step function $\theta(E_F - E(q_x, q_y) - E_z)$. The non-separability of the potential does not allow the energy to be represented by a sum of terms dependent on q_x or q_y alone, so the integrals are performed numerically by evaluating $E(q_x, q_y)$ over a grid of values. The fourth derivatives are obtained using a 9-point difference formula on the energy dispersion. In Fig. 21 we plot $\partial^4 E/\partial q_i^4$ versus q_i, with $0 \leq q_i \leq 1$. Figure 21 displays $\chi_i^{(3)}$ as a function of the number density n of carriers.

As seen from Fig. 22, the optical nonlinearity $\chi_y^{(3)}$ is larger than $\chi_x^{(3)}$, even though $\partial^4 E/\partial q_x^4$ is larger than $\partial^4 E/\partial q_y^4$ (see Fig. 21). A systematic investigation of GaAs/AlGaAs CBSL superlattices[209] over a wide range of well and barrier thicknesses has shown that this can be understood in terms of the scale factors $(a/\pi)^4$ and $(b/\pi)^4$, the effects of band-filling, and the details of the phase-space integrations. The down-turn in $\chi_y^{(3)}$ for number densities above $\sim 10^{18}/cc$ is due to a broad minimum in $\partial^4 E/\partial q_y^4$ at $q_y \sim 0.9$, and which becomes positive near the zone edge. This leads to a partial cancellation in the contribution over the Brillouin zone as the number density pushes the Fermi level to the band edge near the Brillouin zone boundary. The fact that $\chi^{(3)}$ can be lower than in bulk GaAs for certain layer-thickness values has been noted previously by Chang.[208] This is in fact the case for $\chi_{x,y}^{(3)}$ (see Fig. 22) in our particular calculation with the specific choice of

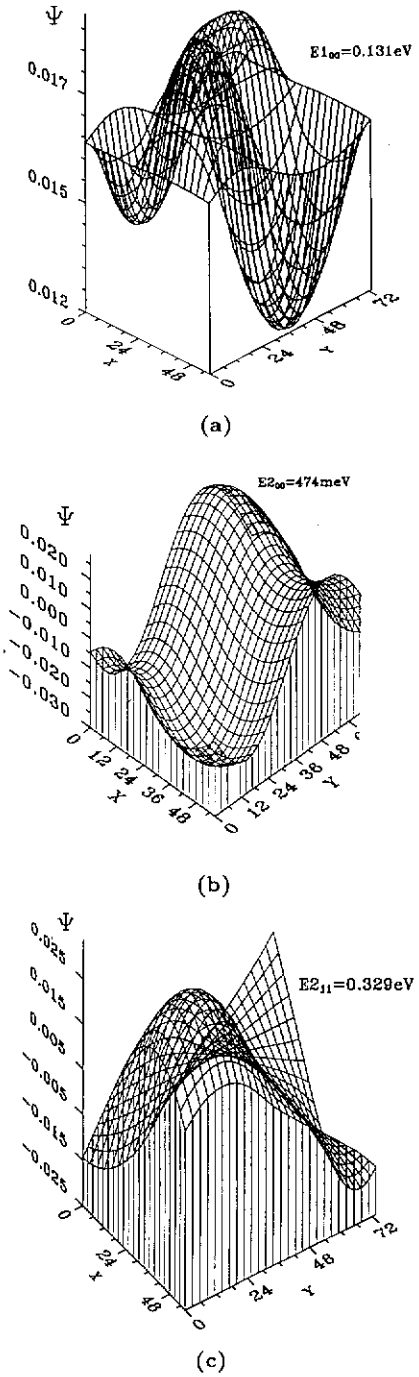

Fig. 20. CBSL conduction electron wavefunctions (a) in the first miniband and (b) in the second miniband, at the zone center. In (c) we show the wavefunction for the second miniband at $(q_x, q_y) = (1, 1)$.

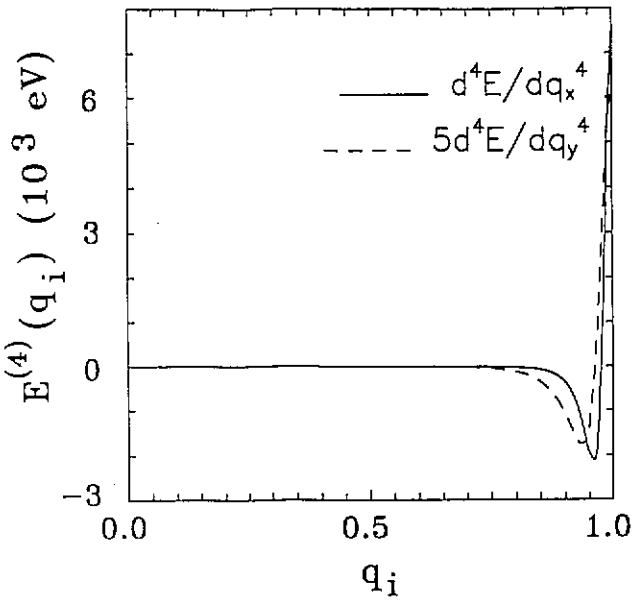

Fig. 21. Fourth derivative of the dispersion for the lowest conduction miniband with respect to (a) q_x (full curve) and (b) q_y (dashed curve) in the CBSL (From Ref. 27).

layer thicknesses for carrier concentrations below $5 \times 10^{17}/cc$ whereas $\chi_y^{(3)}$ is about 1–2 orders of magnitude larger than $\chi_{\text{GaAs}}^{(3)}$ for larger carrier concentrations.

The envelope function approximation has been used extensively to solve for the energy levels and bands in quantum semiconductor heterostructures involving one-dimensional confinement. The FEM permits the use of this approximation in studying structures with 2-dimensional electronic confinement; an extension to periodic structures with non-rectangular geometry is particularly straightforward in the FEM.

We note from Fig. 22 that control over the well and barrier thicknesses (a_1, a_2) and (b_1, b_2) in the two directions can allow for a much broader range of choices for the layer thicknesses in order to increase $\chi^{(3)}$. This is of importance in applications such as intensity dependent optical switching and optical signal processing. Further investigations of the optical and transport properties of CBSLs would be of great theoretical as well as practical interest.

In conclusion, in the proposed new CBSL structure there is an enhancement of $\chi^{(3)}$ over the bulk nonlinearity by about 1–2 orders of magnitude, with the freedom to tailor $\chi^{(3)}$ for each field polarization. The FEM clearly provides the means for doing realistic computations on such complex structures.

6. Concluding Remarks

Recent developments in what we call *wavefunction engineering* of the electronic and optical properties of quantum heterostructures have been reviewed in this work. We

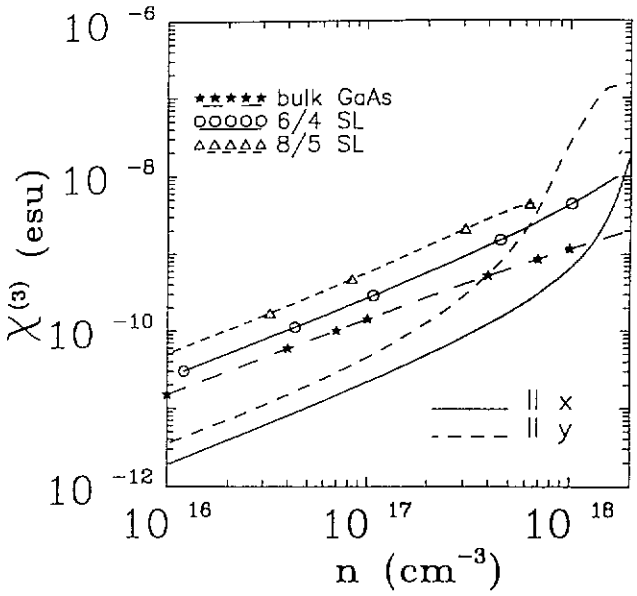

Fig. 22. The free-carrier optical nonlinear susceptibility $\chi^{(3)}$ for the electric vector parallel to $\hat{x}$ (full curve) and $\hat{y}$ (dashed curve). For reference, the values of $\chi^{(3)}$ for bulk GaAs (long-dashed curve with asterisks), for a (6/4) planar superlattice (full curve with open circles), and for an (8/5) superlattice (dashed curve with open triangles) are also shown as functions of carrier density (From Ref. 27).

have emphasized in particular the evolution of the field beyond the more restrictive concept of *bandgap engineering*, in which the confinement of carriers over the physical dimensions of the layers controls the energy gap as a manifestation of Heisenberg's uncertainty relation. Technological advances in the crystal growth of semiconductor heterostructures of III-V and II-VI materials as well as masking and pattern etching, now allow us to much more directly alter the shape of the carrier wavefunctions to suit specific applications. Thus, to a remarkable degree we can control the probability density, or occupancy, of the carriers in any region of the heterostructure. Through the appropriate insertion of thin (even atomic) layers of a different material, by employing asymmetric wells, through the use of type-II interfaces, through localization in the barrier layers for carriers with above-barrier energy, through control over the dynamics of intervalley transfer via externally-applied fields and optical phonon emission, through the use of strain to tailor the band mixing and valence band properties, through the use of diluted magnetic semiconductor layers, and so on, we can significantly alter the carrier wavefunctions. Wavefunction engineering provides a greater appreciation of the mechanisms governing carrier dynamics, since overlap integrals, optical matrix elements, density of states, tunneling times, lifetimes for carrier recombination, optical detection effi-

ciencies, nonlinear optical properties, etc., can now all be altered through a judicious use of 'heterostructure architecture'.

In creating this new generation of advanced devices based on detailed control over the electronic and optical properties of quantum heterostructures with novel geometries, the designer must necessarily rely to a considerable extent on computer modeling of the energy bands and wavefunctions. In the present work, we have demonstrated that the FEM is well suited to the task of efficiently calculating the required properties for structures of arbitrary complexity. Although our emphasis has been on integration of the FEM into the $\mathbf{k}\cdot\mathbf{P}$ framework, it should be mentioned again that tight-binding models may also be viewed in the same context, with individual atoms functioning as the 'finite elements'.

FEM computations have allowed us to explore some fundamental aspects of the band structure of quantum semiconductor systems. The investigations of quasibound states and above-barrier states in III-V heterostructures were driven by modeling and feasibility studies performed with the FEM. The level degeneracy issues in square and rectangular quantum wires with finite barrier height were also revealed through finite element calculations. That we can compute in detail the optical properties of the checkerboard superlattices is based on the ability of the FEM to model complex geometries. By extrapolation, exciting new results revealing new physics can clearly be anticipated with explorations into the properties of systems with 3-D confinement. Wavefunction engineering, made feasible by finite element modeling, will play a vital role in the exploration of new physical concepts and in the development of new devices based on quantum heterostructures.

7. Acknowledgments

We wish to thank F. Bartoli, J. K. Furdyna, C. Hoffman, H. Luo, A. K. Ramdas and J. Shertzer for collaboration on a number of topics presented here. We wish to thank Quantum Semiconductor Algorithms (QSA) for the use of their finite element algorithms. This work was supported by the Office of Naval Research and SDIO/IST managed by NRL.

References

1. L. Esaki and R. Tsu, *IBM J. Res. Dev.* **14**, 61 (1970).
2. R. Dingle, W. Wiegmann and C. H. Henry, *Phys. Rev. Lett.* **33**, 827 (1974).
3. N. Holonyak, Jr., R. M. Kolbas, R. D. Dupuis and P. D. Dapkus, *IEEE J. Quantum Electron.* **16**, 170 (1980).
4. L. L. Chang, L. Esaki and R. Tsu, *Appl. Phys. Lett.* **24**, 593 (1974).
5. E. A. Rezek, H. Shichijo, B. A. Vojak and N. Holonyak, Jr., *Appl. Phys. Lett.* **31**, 534 (1977).
6. W. T. Tsang, *Appl. Phys. Lett.* **39**, 786 (1981).
7. T. Mimura, S. Hiyamizu, T. Fujii and K. Nanbu, *Jpn. J. Appl. Phys.* **19**, L225 (1980).
8. F. Capasso, *J. Vac. Sci. Tech.* **B1**, 457 (1983).
9. F. Capasso, *Surf. Sci.* **142**, 513 (1984).
10. E. Yablonovitch, H. M. Cox and T. J. Gmitter, *Appl. Phys. Lett.* **52**, 1002 (1988).

11. E. P. O'Reilly and A. R. Adams, *IEEE J. Quantum Electron.* **30**, 366 (1994).
12. J. R. Meyer, C. A. Hoffman, F. J. Bartoli, E. R. Youngdale and L. R. Ram-Mohan, *IEEE J. Quantum Electron.*, in press.
13. R. T. Bate and N. G. Einspruch, *Phys. Rev.* **153**, 796 (1967).
14. J. N. Schulman and Y.-C. Chang, *Phys. Rev.* **B27**, 2346 (1983).
15. L. C. Lew Yan Voon and L. R. Ram-Mohan, *Phys. Rev.* **B47**, 15500 (1993).
16. G. Bastard, *Phys. Rev.* **B24**, 5693 (1981).
17. G. Bastard, *Phys. Rev.* **B25**, 7584 (1982).
18. G. Bastard, *Wave Mechanics Applied to Semiconductor Heterostructures*, Les Editions de Physique, Les Ulis (1988).
19. L. R. Ram-Mohan, K. H. Yoo and R. L. Aggarwal, *Phys. Rev.* **B38**, 6151 (1988).
20. K.-J. Bathe, *Finite Element Procedures in Engineering Analysis* (Prentice-Hall, New Jersey, 1982).
21. T. J. R. Hughes, *The Finite Element Method* (Prentice Hall, Englewood Cliffs, 1987).
22. L. R. Ram-Mohan, *Finite Element and Boundary Element Applications in Quantum Mechanics* (Oxford Univ. Press, to appear July 1995).
23. A multiband finite element calculation of superlattice band structures was developed independently by K. Nakamura, A. Shimizu, M. Koshiba and K. Hayata, *IEEE J. Quantum Electron.* **27**, 2035 (1991).
24. L. R. Ram-Mohan, S. Saigal, D. Dossa and J. Shertzer, *Comput. Phys.* **4**, 50 (1990) and references therein.
25. J. Shertzer, L. R. Ram-Mohan and D. Dossa, *Phys. Rev.* **A40**, 4777 (1989).
26. J. Shertzer and L. R. Ram-Mohan, *Phys. Rev.* **B41**, 9994 (1990).
27. L. R. Ram-Mohan and J. Shertzer, *Appl. Phys. Lett.* **57**, 282 (1990).
28. R. Goloskie, J. W. Kramer and L. R. Ram-Mohan, *Computers in Physics* **8**, to appear (1994).
29. M. Gell-Mann and M. Levy, *II Nuov. Cim.* **16**, 53 (1960).
30. W. H. Press, S. A. Teukolsky, W. T. Vetterling and B. R. Flannery, *Numerical Recipes* (Cambridge Univ. Press, 1992).
31. K. H. Yoo, R. L. Aggarwal and L. R. Ram-Mohan, *J. Vac. Sci. Tech.* **A7**, 415 (1989).
32. K. H. Yoo, L. R. Ram-Mohan and D. F. Nelson, *Phys. Rev.* **B39**, 12808 (1989).
33. B. Chen, M. Lazzouni and L. R. Ram-Mohan, *Phys. Rev.* **B45**, 1204 (1992).
34. C. Parks, A. K. Ramdas, M. R. Melloch and L. R. Ram-Mohan, *Phys. Rev.* **B48**, 5413 (1993).
35. M. A. Herman, D. Bimberg and J. Christen, *J. Appl. Phys.* **70**, R1 (1991).
36. R. Nicolini, L. Vanzetti, G. Mula, G. Bratina, L. Sorba, A. Franciosi, M. Peressi, S. Baroni, R. Resta, A. Baldereschi, J. E. Angelo and W. W. Gerberich, *Phys. Rev. Lett.* **72**, 294 (1994).
37. J. R. Meyer, C. A. Hoffman, B. V. Shanabrook, B. R. Bennett, R. J. Wagner, J. R. Waterman and E. R. Youngdale, *Proc. 22nd Int. Conf. Phys. Semicond.*, Vancouver (1994), in press.
38. W. Hansen, J. P. Kotthaus and U. Merkt, in *Semiconductors and Semimetals*, Vol. 35, ed. R. K. Willardson and A. C. Beer (Academic, New York, 1992) chp. 5.
39. Y. Hirayama and H. Okamoto, *Jpn. J. Appl. Phys.* **24**, L965 (1985).
40. K. Kash, J. M. Worlock, M. D. Sturge, P. Grabbe, J. P. Harbison, A. Scherer and P. S. D. Lin, *Appl. Phys. Lett.* **53**, 782 (1988).
41. M. Grundmann, E. Kapon, J. Christen and D. Bimberg, *J. Nonlin. Opt. Phys. Mat.*, in press (this issue).
42. L. Pfeiffer, H. L. Stormer, K. W. Baldwin, K. W. West, A. R. Goni, A. Pinczuk, R. C. Ashoori, M. M. Dignam and W. Wegscheider, *J. Cryst. Growth* **127**, 849 (1993).

43. M. Tsuchiya, J. M. Gaines, R. H. Yan, R. J. Simes, P. O. Holtz, L. A. Coldren and P. M. Petroff, *Phys. Rev. Lett.* **62**, 466 (1989).
44. F. Capasso, K. Mohammed and A. Y. Cho, *IEEE J. Quantum Electron.* **22**, 1853 (1986).
45. F. Capasso, S. Sen, F. Beltram, L. M. Lunardi, A. S. Vengurlekar, P. R. Smith, N. J. Shah, R. J. Malik and A. Y. Cho, *IEEE Trans. Electron Dev.* **36**, 2065 (1989).
46. E. P. O'Reilly, *Semicond. Sci. Tech.* **1**, 121 (1989).
47. C. Weisbuch, *J. Cryst. Growth* **127**, 742 (1993).
48. H. Sakaki, *Solid State Comm.* **92**, 119 (1994).
49. D. A. B. Miller, *Opt. Quantum Electron.* **22**, S61 (1990).
50. D. S. Chemla, D. A. B. Miller, P. W. Smith, A. C. Gossard and W. Wiegman, *IEEE J. Quantum Electron.* **20**, 265 (1984).
51. R. Tsu and L. Esaki, *Appl. Phys. Lett.* **22**, 562 (1973).
52. J. N. Schulman and T. C. McGill, *Appl. Phys. Lett.* **34**, 663 (1979).
53. T. H. Myers, J. R. Meyer, C. A. Hoffman and L. R. Ram-Mohan, *Appl. Phys. Lett.* **61**, 1814 (1992).
54. A. Kastalsky, T. Duffield, S. J. Allen and J. Harbison, *Appl. Phys. Lett.* **52**, 1320 (1988).
55. S. S. Li, M. Y. Chuang and L. S. Yu, *Semicond. Sci. Tech.* **8**, S406 (1993).
56. E. O. Kane, *J. Phys. Chem. Solids* **1**, 249 (1957).
57. J. M. Perez, R. J. Wagner, J. R. Meyer, J. W. Han, J. W. Cook, Jr. and J. F. Schetzina, *Phys. Rev. Lett.* **61**, 2261 (1988).
58. G. C. Osbourn, *J. Vac. Sci. Tech.* **B1**, 379 (1983).
59. Y. H. Wang, S. S. Li, J. Chu and P. Ho, *Appl. Phys. Lett.* **64**, 727 (1994).
60. C. J. Summers and K. F. Brennan, *Appl. Phys. Lett.* **48**, 806 (1986).
61. R. F. Kazarinov and R. A. Suris, *Fiz. Tekh. Polupov.* **5**, 797 (1971) [*Sov. Phys. Semicond.* **5**, 707 (1971)].
62. J. Faist, F. Capasso, D. L. Sivco, C. Sirtori, A. L. Hutchinson and A. Y. Cho, *Science* **264**, 553 (1994).
63. S. Y. Yuen, *Appl. Phys. Lett.* **41**, 590 (1982).
64. F. Capasso, C. Sirtori and A. Y. Cho, *IEEE J. Quantum Electron.* **30**, 1313 (1994).
65. L. C. Lew Yan Voon and L. R. Ram-Mohan, *Phys. Rev.* **B50** (Nov. 1994).
66. M. Sh. Aidaraliev, G. G. Zegrya, N. V. Zotova, S. A. Karandashev, B. A. Matveev, N. M. Stus' and G. N. Talalakin, *Fiz. Tekh. Poluprov.* **26**, 246 (1992) [*Sov. Phys. Semicond.* **26**, 138 (1992)].
67. Y. Jiang, M. C. Teich, W. I. Wang and J. R. Meyer, *J. Appl. Phys.* **71**, 3394 (1992).
68. J. L. Pan, *Phys. Rev.* **B46**, 3977 (1992).
69. P. L. Gourley, J. R. Wendt, G. A. Vawter, T. M. Brennan and B. E. Hammons, *Appl. Phys. Lett.* **64**, 687 (1994).
70. A. M. Glass, D. D. Nolte, D. H. Olsen, G. E. Doran, D. S. Chemla and W. H. Knox, *Opt. Lett.* **15**, 264 (1990).
71. S. J. Pearton and N. J. Shah, in *High-Speed Semiconductor Devices*, ed. S. M. Sze (Wiley, New York, 1990) chp. 5.
72. A. G. Markelz, E. G. Gwinn, M. S. Sherwin, C. Nguyen and H. Kroemer, *Solid-State Electron.* **37**, 1243 (1994).
73. C. Sirtori, F. Capasso, J. Faist, L. N. Pfeiffer and K. W. West, *Appl. Phys. Lett.* **65**, 445 (1994).
74. L. C. Lew Yan Voon and L. R. Ram-Mohan, submitted to *Appl. Phys. Lett.*
75. C.-L. Yang and D.-S. Pan, *J. Appl. Phys.* **64**, 1573 (1988).

76. M. Heiblum, E. Calleja, I. M. Anderson, W. P. Dumke, C. M. Knoedler and L. Osterling, *Phys. Rev. Lett.* **56**, 2854 (1986).
77. R. P. G. Karunasiri, J. S. Park, K. L. Wang and L.-J. Cheng, *Appl. Phys. Lett.* **56**, 1342 (1990).
78. Y. H. Wang, S. S. Li, P. Ho and M. O. Manasreh, *J. Appl. Phys.* **74**, 1382 (1993).
79. E. R. Brown, S. J. Eglash and K. A. McIntosh, *Phys. Rev.* **B46**, 7244 (1992).
80. L. A. Samoska, B. Brar and H. Kroemer, *Appl. Phys. Lett.* **62**, 2539 (1993).
81. Y. Zhang, N. Baruch and W. I. Wang, *Appl. Phys. Lett.* **63**, 1068 (1993).
82. H. Xie, W. I. Wang, J. R. Meyer, C. A. Hoffman and F. J. Bartoli, *J. Appl. Phys.* **74**, 1194 (1993).
83. H. Xie, W.-I. Wang, J. R. Meyer and L. R. Ram-Mohan, *Appl. Phys. Lett.* **65**, 2048 (1994).
84. J. R. Meyer, C. A. Hoffman, F. J. Bartoli, H. Xie, W. I. Wang and L. R. Ram-Mohan, submitted to *IEEE J. Quantum Electron.*
85. A. R. Bonnefoi, T. C. McGill, R. D. Burnham and G. B. Anderson, *Appl. Phys. Lett.* **50**, 344 (1987).
86. E. E. Mendez, E. Calleja and W. I. Wang, *Appl. Phys. Lett.* **53**, 977 (1988).
87. O. E. Raichev, *Fiz. Tekh. Poluprov.* **25**, 1228 (1991) [*Sov. Phys. Semicond.* **25**, 740 (1991)].
88. G. A. Sai-Halasz, R. Tsu and L. Esaki, *Appl. Phys. Lett.* **30**, 651 (1977).
89. B. A. Wilson, *IEEE J. Quantum Electron.* **24**, 1763 (1988).
90. J. R. Meyer, C. A. Hoffman, F. J. Bartoli and L. R. Ram-Mohan, *Phys. Rev.* **B49**, 2197 (1994).
91. G. R. Olbright, W. S. Fu, J. F. Klem, H. M. Gibbs, G. Khitrova, R. Pon, B. Fluegel, K. Meissner, N. Peyghambarian, R. Binder, I. Galbraith and S. W. Koch, *Phys. Rev.* **B44**, 3043 (1991).
92. G. Danan, F. R. Ladan, F. Mollot and R. Planel, *J. de Phys.* **48**, C5–499 (1987).
93. D. Gershoni, H. Temkin, J. M. Vandenberg, S. N. G. Chu, R. A. Hamm and M. B. Panish, *Phys. Rev. Lett.* **60**, 448 (1988).
94. R. P. G. Karunasiri and K. L. Wang, *J. Vac. Sci. Tech.* **B9**, 2064 (1991).
95. M.-H. Meynadier, R. E. Nahory, J. M. Worlock, M. C. Tamargo, J. L. de Miguel and M. D. Sturge, *Phys. Rev. Lett.* **60**, 1338 (1988).
96. J. E. Golub, P. F. Liao, D. J. Eilenberger, J. P. Harbison, L. T. Florez and Y. Prior, *Appl. Phys. Lett.* **53**, 2584 (1988).
97. E. R. Youngdale, J. R. Meyer, C. A. Hoffman, F. J. Bartoli and W. I. Wang, *Int. J. Nonlin. Opt. Phys.* **2**, 415 (1993).
98. B. A. Wilson, C. E. Bonner, R. C. Spitzer, P. Dawson, K. J. Moore and C. T. Foxon, *J. Vac. Sci. Tech.* **B6**, 1156 (1988).
99. G. R. Olbright, J. Klem, A. Owyoung, T. M. Brennan, R. Binder and S. W. Koch, *J. Opt. Soc. Am.* **B7**, 1473 (1990).
100. G. A. Sai-Halasz, L. L. Chang, J.-M. Welter, C.-A. Chang and L. Esaki, *Solid State Comm.* **27**, 935 (1978).
101. L. F. Luo, R. Beresford and W. I. Wang, *Appl. Phys. Lett.* **55**, 2023 (1989).
102. J. R. Soderstrom, D. H. Chow and T. C. McGill, *Appl. Phys. Lett.* **55**, 1094 (1989).
103. J. F. Chen, M. C. Wu, L. Yang and A. Y. Cho, *J. Appl. Phys.* **68**, 3040 (1990).
104. D. L. Smith and C. Mailhiot, *J. Appl. Phys.* **62**, 2545 (1987).
105. R. H. Miles, D. H. Chow, J. N. Schulman and T. C. McGill, *Appl. Phys. Lett.* **57**, 801 (1990).
106. C. H. Grein, P. M. Young and H. Ehrenreich, *J. Appl. Phys.* **76**, 1940 (1994).

107. R. H. Miles, D. H. Chow, Y.-H. Zhang and P. D. Brewer, submitted to *Appl. Phys. Lett.*
108. J. R. Meyer, C. A. Hoffman, T. D. Golding, J. T. Zborowski, and A. Vigliante, *Proc. 22nd Int. Conf. Phys. Semicond.*, Vancouver (1994) in press.
109. S. Luryi, A. Kastalsky, A. C. Gossard and R. H. Hendel, *IEEE Trans. Electron. Dev.* **31**, 832 (1984).
110. D. A. B. Miller, D. S. Chemla, D. J. Eilenberger, P. W. Smith, A. C. Gossard and W. T. Tsang, *Appl. Phys. Lett.* **41**, 679 (1982).
111. J. E. Cunningham, *J. Nonlin. Opt. Phys. Mat.* **4**, next issue.
112. G. Bastard, *Phys. Rev.* **B24**, 4714 (1981).
113. J. Bleuse, P. Voisin, M. Allovon and M. Quillec, *Appl. Phys. Lett.* **53**, 2632 (1988).
114. E. Bigan, M. Allovon, M. Carre, C. Braud, A. Carenco and P. Voisin, *IEEE J. Quantum Electron.* **28**, 214 (1992).
115. M. Wegener, T. Y. Chang, I. Bar-Joseph, J. M. Kuo and D. S. Chemla, *Appl. Phys. Lett.* **55**, 583 (1989).
116. G. Lenz and J. Salzman, *Appl. Phys. Lett.* **56**, 871 (1990).
117. E. Rosencher and Ph. Bois, *Phys. Rev.* **B44**, 11315 (1991).
118. V. Berger, N. Vodjdani, B. Vinter, E. Costard and E. Bockenhoff, *Appl. Phys. Lett.* **60**, 1869 (1992).
119. F. C. Zhang, N. Dai, H. Luo, N. Samarth, M. Dobrowolska, J. K. Furdyna and L. R. Ram-Mohan, *Phys. Rev. Lett.* **68**, 3220 (1992).
120. C. Sirtori, F. Capasso, D. L. Sivco and A. Y. Cho, *Appl. Phys. Lett.* **64**, 2982 (1994).
121. A. Sasaki, *Phys. Rev.* **B30**, 7016 (1984).
122. R. E. Doezema and H. D. Drew, *Phys. Rev. Lett.* **57**, 762 (1986).
123. M. Kubisa and W. Zawadzki, *Semicond. Sci. Tech.* **8**, S246 (1993).
124. D. A. B. Miller, D. S. Chemla, T. C. Damen, A. C. Gossard, W. Wiegmann, T. H. Wood and C. A. Burrus, *Phys. Rev. Lett.* **53**, 2173 (1984).
125. P. F. Yuh and K. L. Wang, *IEEE J. Quantum Electron.* **25**, 1671 (1989).
126. M. Morita, K. Goto and T. Suzuki, *Jpn. J. Appl. Phys.* **29**, L1663 (1990).
127. S. R. Parihar, S. A. Lyon, M. Santos and M. Shayegan, *Appl. Phys. Lett.* **55**, 2417 (1989).
128. B. F. Levine, C. G. Bethea, V. O. Shen and R. J. Malik, *Appl. Phys. Lett.* **57**, 383 (1990).
129. D. A. Holm and H. F. Taylor, *IEEE J. Quantum Electron.* **25**, 2266 (1989).
130. M. Seto and M. Helm, *Appl. Phys. Lett.* **60**, 859 (1992).
131. P. F. Yuh and K. L. Wang, *J. Appl. Phys.* **65**, 4377 (1989).
132. F. M. Peeters and P. Vasilopoulos, *Appl. Phys. Lett.* **55**, 1106 (1989).
133. P. Vasilopoulos, F. M. Peeters and D. Aitelhabti, *Phys. Rev.* **B41**, 10021 (1990).
134. T. Tsuchiya and T. Ando, *Phys. Rev.* **B48**, 4599 (1993).
135. T. Akazaki, J. Nitta, H. Takayanagi, T. Enoki and K. Arai, *Appl. Phys. Lett.* **65**, 1263 (1994).
136. K. Ensslin, D. Heitmann and K. Ploog, *Appl. Phys. Lett.* **55**, 368 (1989).
137. W. O. Chen and T. G. Andersson, *J. Appl. Phys.* **73**, 4484 (1993).
138. J. S. Yoo and H. H. Lee, *J. Appl. Phys.* **71**, 518 (1992).
139. M. S. Kiledjian, J. N. Schulman and K. L. Wang, *Phys. Rev.* **B44**, 5616 (1991).
140. W. Trzeciakowski and B. D. McCombe, *Appl. Phys. Lett.* **55**, 891 (1989).
141. W. J. Li, S. Holmes, W. Trzeciakowski, B. D. McCombe, X. Liu, A. Petrou, M. Dutta, P. G. Newman and W. Schaff, *Superlatt. Microstruct.* **8**, 163 (1990).
142. H. Schneider, F. Fuchs, B. Dischler, J. D. Ralston and P. Koidl, *Appl. Phys. Lett.* **58**, 2234 (1991).

143. M. Sato and Y. Horikoshi, *Appl. Phys. Lett.* **56**, 1555 (1990).
144. G. Ihm, S. K. Noh, J. I. Lee, J.-S. Hwang and T. W. Kim, *Phys. Rev.* **B44**, 6266 (1991).
145. F. Beltram and F. Capasso, *Phys. Rev.* **B38**, 3580 (1988).
146. W. T. Masselink, *Phys. Rev. Lett.* **66**, 1513 (1991).
147. Y. Arakawa and H. Sakaki, *Appl. Phys. Lett.* **40**, 939 (1982).
148. E. Kapon, S. Simhony, R. Bhat and D. M. Hwang, *Appl. Phys. Lett.* **55**, 2715 (1989).
149. M. A. Reed, J. N. Randall, R. J. Aggarwal, R. J. Matyi, T. M. Moore and A. E. Wetsel, *Phys. Rev. Lett.* **60** (1988).
150. A. C. Seabaugh, J. H. Luscombe and J. N. Randall, *Fut. Electron. Dev. J. Jpn.* **2**, No. 3 (1992).
151. Y.-C. Chang, L. L. Chang and L. Esaki, *Appl. Phys. Lett.* **47**, 1324 (1985).
152. D. S. Citrin, *Int. J. Nonlin. Opt. Phys.* **4**, this issue.
153. H. Benisty, C. Sotomayor-Torres and C. Weisbuch, *Phys. Rev.* **B44**, 10945 (1991).
154. I. Vurgaftman and J. Singh, *Appl. Phys. Lett.* **64**, 232 (1994).
155. H. Sakaki, *Surf. Sci.* **267**, 623 (1992).
156. R. A. Abram, R. W. Kelsall and R. I. Taylor, *J. Phys. Chem. Sol.* **49**, 607 (1988).
157. H. K. Choi and S. J. Eglash, *Appl. Phys. Lett.* **61**, 1154 (1992).
158. M. Aidaraliev, N. V. Zotova, S. A. Karandashev, B. A. Matveev, N. M. Stus' and G. N. Talalakin, *Fiz. Tekh. Poluprov.* **27**, 21 (1993) [*Sov. Phys. Semicond.* **27**, 10 (1993)].
159. S. J. Eglash and H. K. Choi, *Appl. Phys. Lett.* **64**, 833 (1994).
160. S. R. Kurtz, R. M. Biefeld, L. R. Dawson, K. C. Baucom and A. J. Howard, *Appl. Phys. Lett.* **64**, 812 (1994).
161. A. N. Baranov, A. N. Imenkov, V. V. Shertstnev and Yu. P. Yakovlev, *Appl. Phys. Lett.* **64**, 2480 (1994).
162. H. K. Choi, S. J. Eglash and G. W. Turner, *Appl. Phys. Lett.* **64**, 2474 (1994).
163. Y. Tsou, A. Ichii and E. M. Garmire, *IEEE J. Quantum Electron.* **28**, 1261 (1992).
164. Y. Horikoshi, *Semiconductors and Semimetals*, Vol. 22C, ed. W. T. Tsang (Academic, New York, 1985) chp. 3.
165. A. I. Andrushko, Kh. M. Salikhov and S. V. Slobodchikov, *Fiz. Tekh. Poluprov.* **20**, 403 (1986) [*Sov. Phys. Semicond.* **20**, 255 (1986)].
166. E. R. Youngdale, J. R. Meyer, C. A. Hoffman, F. J. Bartoli, C. H. Grein, P. M. Young, H. Ehrenreich, R. H. Miles and D. H. Chow, *Appl. Phys. Lett.* **64**, 3160 (1994).
167. Although the sample studied in Ref. 166 had a cut-off wavelength somewhat beyond the MWIR (8.9 μm), recent experiments on a non-optimized InAs-$Ga_{1-x}In_xSb$ superlattice grown at NRL confirmed that the Auger lifetime for $\lambda_c = 4.8$ μm at 300 K was enhanced by more than a factor of 3 over any obtained previously for a III-V or II-VI semiconductor with equivalent energy gap (E. R. Youngdale, J. R. Meyer, C. A. Hoffman, B. R. Bennett, J. R. Waterman, B. V. Shanabrook and R. J. Wagner, unpublished data).
168. W. T. Tsang, *Semiconductor and Semimetals*, Vol. 24, ed. R. Dingle (Academic, New York, 1987) chp. 7.
169. M. M. Fejer, S. J. B. Yoo, R. L. Byer, A. Harwit and J. S. Harris, Jr., *Phys. Rev. Lett.* **62**, 1041 (1989).
170. C. Sirtori, F. Capasso, D. L. Sivco, S. N. G. Chu and A. Y. Cho, *Appl. Phys. Lett.* **59**, 2302 (1991).
171. J. Khurgin, *J. Opt. Soc. Am.* **B6**, 1673 (1989).
172. D. J. Erskine, A. J. Taylor and C. L. Tang, *Appl. Phys. Lett.* **45**, 54 (1984).

173. P. C. Becker, H. L. Fragnito, C. H. Brito Cruz, J. Shah, R. L. Fork, J. E. Cunningham, J. E. Henry and C. V. Shank, *Appl. Phys. Lett.* **53**, 2089 (1988).
174. J. L. Educato and J. P. Leburton, *Phys. Rev.* **B49**, 2177 (1994).
175. S. M. Goodnick and J. E. Lary, *Semicond. Sci. Tech.* **7**, B109 (1992).
176. E. Rosencher, *J. Appl. Phys.* **73**, 1909 (1993).
177. D. Dossa, L. C. Lew Yan Voon, L. R. Ram-Mohan, C. Parks, R. G. Alonso, A. K. Ramdas and M. R. Melloch, *Appl. Phys. Lett.* **59**, 2706 (1991).
178. C. Parks, A. K. Ramdas, M. R. Melloch, G. Steblovsky, L. R. Ram-Mohan and H. Luo, *Solid State Comm.* **92**, 563 (1994).
179. C. Parks, R. G. Alonso, A. K. Ramdas, L. R. Ram-Mohan, D. Dossa and M. R. Melloch, *Phys. Rev.* **B24**, 14215 (1992).
180. J. M. Moison, K. Elcess, F. Houzay, J. Y. Marzin, J. M. Gerard, F. Barthe and M. Bensoussan, *Phys. Rev.* **B41**, 12945 (1990).
181. R. M. Cohen, M. Kitamura and Z. M. Fang, *Appl. Phys. Lett.* **50**, 1675 (1987).
182. E. Yablonovitch and E. O. Kane, *J. Lightwave Tech.* **6**, 1292 (1988).
183. Z. Sobiesierski, S. A. Clark and R. H. Williams, *Appl. Surf. Sci.* **56**, 703 (1992).
184. Y. R. Lee, A. K. Ramdas, F. A. Chambers, J. M. Meese and L. R. Ram-Mohan, *Appl. Phys. Lett.* **50**, 600 (1987).
185. O. J. Glembocki and B. V. Shanabrook, *Semiconductors and Semimetals*, Vol. 36, ed. R. K. Willardson, A. C. Beer and E. R. Weber (Academic, San Diego, 1992) pp. 222.
186. H. Luo, L. R. Ram-Mohan, G. L. Yang and J. K. Furdyna, *J. Electron. Mat.* **22**, 1103 (1993).
187. L. C. Lew Yan Voon, L. R. Ram-Mohan, H. Luo and J. K. Furdyna, *Phys. Rev.* **B47**, 6585 (1993).
188. N. Dai, L. R. Ram-Mohan, H. Luo, G. L. Yang, F. C. Zhang, M. Dobrowolska and J. K. Furdyna, submitted for publication (1994).
189. *Landolt-Börnstein, Numerical Data and Functional Relationships in Science and Technology*, ed. O. Madelung (Springer, Berlin, 1982), Gp. III, Vol. 17.
190. D. F. Nelson, R. C. Miller, C. W. Tu and S. K. Sputz, *Phys. Rev.* **B36**, 8063 (1987).
191. W. Trzeciakowski and M. Gurioli, *Phys. Rev.* **B44**, 3880 (1991).
192. H. Sakaki, *Jpn. J. Appl. Phys.* **19**, L735 (1980).
193. P. M. Petroff, A. C. Gossard, R. A. Logan and W. Wiegmann, *Appl. Phys. Lett.* **41**, 635 (1982).
194. J. Cibert, P. M. Petroff, G. J. Dolan, S. J. Pearton, A. C. Gossard and J. H. English, *Appl. Phys. Lett.* **49**, 1275 (1986).
195. H. Temkin, G. J. Dolan, M. B. Panish and S. N. G. Chu, *Appl. Phys. Lett.* **50**, 413 (1987).
196. E. Kapon, D. M. Hwang and R. Bhat, *Phys. Rev. Lett.* **63**, 430 (1989).
197. J. Lee, *J. Appl. Phys.* **54**, 5482 (1983).
198. H. H. Hassan and H. N. Spector, *J. Vac. Sci. Tech.* **A3**, 22 (1985).
199. H. S. Cho and P. R. Prucnal, *Phys. Rev.* **B39**, 11150 (1989).
200. D. A. B. Miller, D. S. Chemla and S. Schmitt-Rink, *Appl. Phys. Lett.* **52**, 2154 (1988).
201. K. B. Wong, M. Jaros and J. P. Hagon, *Phys. Rev.* **B35**, 2463 (1987).
202. K. S. Dy and S.-Y. Wu, *Phys. Rev.* **B38**, 5709 (1988).
203. M. Tinkham, *Group Theory and Quantum Mechanics* (McGraw Hill, New York, 1964) pp. 325–329.
204. C. K. N. Patel, R. E. Slusher and P. A. Fleury, *Phys. Rev. Lett.* **17**, 1011 (1966).
205. P. A. Wolff and G. A. Pearson, *Phys. Rev. Lett.* **17**, 1015 (1966).
206. W. L. Bloss and L. Friedman, *Appl. Phys. Lett.* **41**, 1023 (1982).

207. G. Cooperman, L. Friedman and W. L. Bloss, *Appl. Phys. Lett.* **44**, 977 (1984).
208. Y.-C. Chang, *J. Appl. Phys.* **58**, 499 (1985).
209. H. Xie, L. R. Ram-Mohan and L. R. Friedman, *Phys. Rev.* **B42**, 7124 (1990).
210. J. R. Meyer, F. J. Bartoli, E. R. Youngdale and C. A. Hoffman, *J. Appl. Phys.* **70**, 4317 (1991).